Development of Electroless Silver Plating on *Para*-Aramid Fibers and Growth Morphology of Silver Deposits

Huiru Zhang, Xinguo Zou, Jingjing Liang, Xiao Ma, Zhiyong Tang, Jinliang Sun

Research Center for Composite Materials, School of Materials Science and Engineering, Shanghai University, Shanghai 200072, People's Republic of China

Received 10 May 2011; accepted 23 July 2011
DOI 10.1002/app.35332
Published online 21 November 2011 in Wiley Online Library (wileyonlinelibrary.com).

ABSTRACT: The development of a conductive fiber with flame resistance is an urgent concern particularly in national defense and other specialized fields. Aramid fibers (*para*- or *meta*-) exihibit high strength and excellent fire resistance. Electroless silver plating on *para*-aramid fibers and growth morphology of silver deposits was investigated in the present work. The surface of *para*-aramid fibers was roughened using sodium hydride/dimethyl sulfoxide to guarantee successful electroless plating. Two complexing agents (ethylene diamine/ammonia) and two reducing agents (glucose/seignette salt) were used for the electroless silver plating bath design. Structure and properties of the resulting silver-deposited *para*-aramid fibers were evaluated based on scanning electron microscopy, silver weight gain percentage calculation, electrical resistance measurement, crystal structure analysis, and mechanical properties test. The results showed that a higher silver weight gain was advantageous to the improvement of conductivity for the silver-deposited *para*-aramid fibers. The obtained silver deposit was homogenous and compact. Electroless silver-plating deposits were considered to be three-dimensional nucleation and growth model (Volmer–Weber). Black, silver gray, and white deposits appeared sequentially with progressive plating. The breaking strength of silver-deposited *para*-aramid fibers remained at value up to 44 N. © 2011 Wiley Periodicals, Inc. J Appl Polym Sci 124: 3363–3371, 2012

Key words: *para*-aramid; electroless silver plating; silver weight gain percentage; surface morphology; growth morphology

INTRODUCTION

Polyamide (nylon), polyester (terylene), polyurethane (spandex), etc., are the conventional substrate materials used in conductive fibers. The common problem with these fibers is the low melting temperature resulting in adverse effects, such as burning, which limits their application. This problem highlights the urgency of developing a conductive fiber with flame resistance and a no-melt, no-drip performance. Aramid fibers (*para*-aramid and *meta*-aramid) have excellent flame resistance and high strength, which were chosen as substrate materials to produce conductive fibers by electroless plating of silver in the present work.

Compared to sputtering and electro-deposition, electroless plating is the most preferred method for producing metal deposit on fibers. Its advantages are flexibility, excellent conductivity, and applicability to nonconductors or components with complex geometry. It can also be applied to almost all kinds of fibers.

Consequently, metal-deposited *para*-aramid fibers obtained by electroless plating have attracted the attention of researchers. The excellent characteristics of *para*-aramid fibers have led to their wide applications in many fields, such as electronics, aeronautics/astronautics, aircraft, modern fighter, fire fighting, and national defense.

Electroless plating of metals on *para*-aramid fibers has been the subject of a significant number of studies. Burch[1] used strong bases, whereas Gabara[2] used sulfonic acid to etch *para*-aramid surface. Hsu[3,4] used nitric acid, chlorosulfonic acid, and fluorosulfonic acid to etch *para*-aramid surface, respectively. Subsequently, it was performed electroless plating on *para*-aramid fibers. Xi[5] used palladium (II)-hexafluoroacetylacetonate [$Pd(hfa)_2$] as pretreatment agent and adopted the supercritical fluid technology to treat *para*-aramid surface and perform electroless plating of copper on *para*-aramid fibers. Burch[6] added polyvinyl pyrrolidone in the electroless plating bath to enhance the binding between *para*-aramid and metal deposits. Kosuga[7] used silane-coupling agent chelating metal palladium to activate the *para*-aramid surface for electroless plating of metal alloy on *para*-aramid fibers. Banaszczyk[8] prepared and studied the two polypyrrole-coated woven para-aramid fabrics. Schwarz and Gasana[9,10] reported the

Correspondence to: H. Zhang (zhanghuiru@shu.edu.cn).
Contract grant sponsor: National Natural Science Foundation of China (NFSC); contract grant number: 51103083.
Contract grant sponsor: Shanghai Leading Academic Discipline Project; contract grant number: s30107.

TABLE I
Surface Pretreatment of *Para*-Aramid Fibers

Steps	Conditions	Temperature (°C)	Time /min
Degreasing	Acetone	Room temperature	60
Coarsening	5 g NaH, 150 g DMSO	30	10
Sensitizing	$SnCl_2$ 20 g/L, HCl (36%) 20 mL/L	30	10
Activating	$PdCl_2$ 0.33 g/L, HCl (36%) 4 mL/L	30	10
Neutralizing	NaOH 10 g/L	Room temperature	2

electroless deposition of copper on polypyrrole-modified surfaces of *para*-aramid yarns. Schwarz[11] described electroless deposition of gold on the polypyrrole/copper-modified surface of *para*-aramid yarns.

In the present work, *para*-aramid surfaces were etched by sodium hydride/dimethyl sulfoxide (NaH/DMSO) coarsening solution to guarantee electroless plating of silver on *para*-aramid. Two complexing agents (ethylene diamine/ammonia) and two reducing agents (glucose/seignette salt) were used for the electroless silver plating bath design. Structure and properties of the resulting silver-deposited *para*-aramid fibers were studied by scanning electron microscopy (SEM), silver weight gain percentage calculation, electrical resistance measurement, crystal structure analysis, and mechanical properties test. In addition, the effect of plating time on the growth morphology of the silver deposit was also investigated.

EXPERIMENTAL

Materials

Substrate material: *para*-aramid (Kevlar 29 200 days, DuPont).

Chemical agents: DMSO, sodium hydride (NaH, 60% ± 5%), acetone (CH_3COCH_3), stannous chloride ($SnCl_2$), palladous chloride ($PdCl_2$), hydrochloric acid (HCl, 36–38%), sodium hydroxide (NaOH), silver nitrate ($AgNO_3$), ammonia ($NH_3{\cdot}H_2O$), ethylene diamine ($C_2H_8N_2$), potassium hydroxide (KOH), glucose ($C_6H_{12}O_6$), seignette salt ($C_4H_4O_6KNa{\cdot}4H_2O$), ethanol (C_2H_5OH), and polyethylene glycol 1000 (PEG1000). All the reagents were of analytical grade and purchased from Sinopharm Chemical Reagent Co. (Shanghai, China).

Preparation of electroless silver plating on *para*-aramid fibers

Pretreatment step

Commercial *para*-aramid shows a smooth surface, low reactivity, and high degree of crystallinity. Therefore, the surface of *para*-aramid must be pretreated before electroless plating. The pretreatment involves degreasing, coarsening, sensitizing, activating, and neutralizing. The pretreatment steps and conditions are listed in Table I.

Electroless silver plating bath composition

Electroless silver plating on surface-modified *para*-aramid fibers was developed. The optimized composition and operating conditions of the silver plating solution are given in Table II. These values were obtained from optimization experiments. In these experiments, silver nitrate was the silver salt. Ammonia and ethylene diamine were the complexing agents. Potassium hydroxide was the velocity regulator. Glucose and seignette salt were the reducing agents. Ethanol and polyethylene glycol 1000 were the additives.

Characterization

Weight gain percentage calculation

The weight gain percentage is calculated using the following formula:

$$\text{Weight gain percentage} = [(m_2 - m_1)/m_1] \times 100\% \quad (1)$$

TABLE II
Composition of Electroless Silver Plating Bath and Operating Conditions

	Composition (g/L)	
Silver ion complexing solution	Silver nitrate	10
	Ammonia	40–200 ml/L
	Ethylene diamine	0–30 ml/L
	Potassium hydroxide	6
Reductive solution	Glucose	0–20
	Seignette salt	0–10
	Ethanol	40 ml/L
	Polyethylene glycol 1000	75 ml/L
Operating conditions	Temperature	25–30°C
	Plating time	70 min

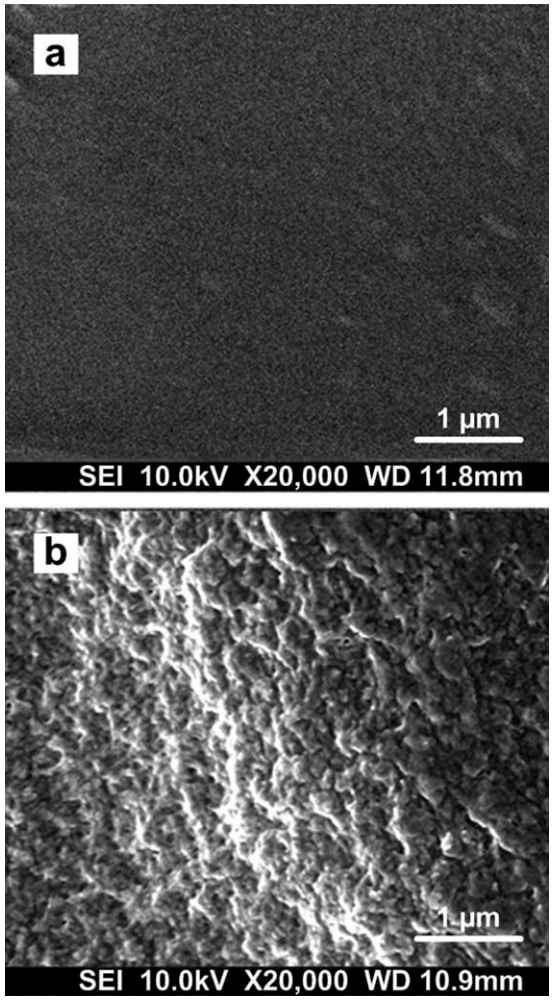

Figure 1 SEM photographs of *para*-aramid fibers without and with etching (a) without etching (b) with etching.

where m_1 and m_2 are the mass (g) of *para*-aramid fibers before and after silver deposited, respectively.

Mechanical properties test

The mechanical properties of the electroless silver-deposit *para*-aramid fibers were evaluated based on the GB/T 14344-2008 standard (testing method for tensile of man-made filament yarns). The measurements were carried out by Jiangsu Provincial Textile Research Institute Co. The sample length was 500 mm, and an extension rate of 250 mm/min was adopted. For each specimen, 20 individual measurements were performed at a temperature of 20°C as well as a relative humidity of 65%.

Electrical resistance test

Electrical resistances of the silver-deposit *para*-aramid fibers were measured using a multitester (Fluke15B). The sample length was 20 cm. Similar with the mechanical properties test, 20 individual measurements of electrical resistance were performed for each specimen at the room temperature.

SEM observation

The surface morphology of the silver-deposit *para*-aramid fibers was observed using a JSM-6700F scanning electric microscope (SEM, JEOL Co., Japan). Furthermore, the grain size of silver deposits was measured by the image processing of the JEOL Smile View software.

XRD analysis

X-ray diffraction (XRD) analysis was performed using a DLMAX-2550 analyzer (Rigaku, Japan) with a scan velocity of 8°/min and a scan range of 30°–90°. The crystallite size and the crystal plane texture coefficients (TC) of the silver deposits were estimated according to the following equations, respectively:

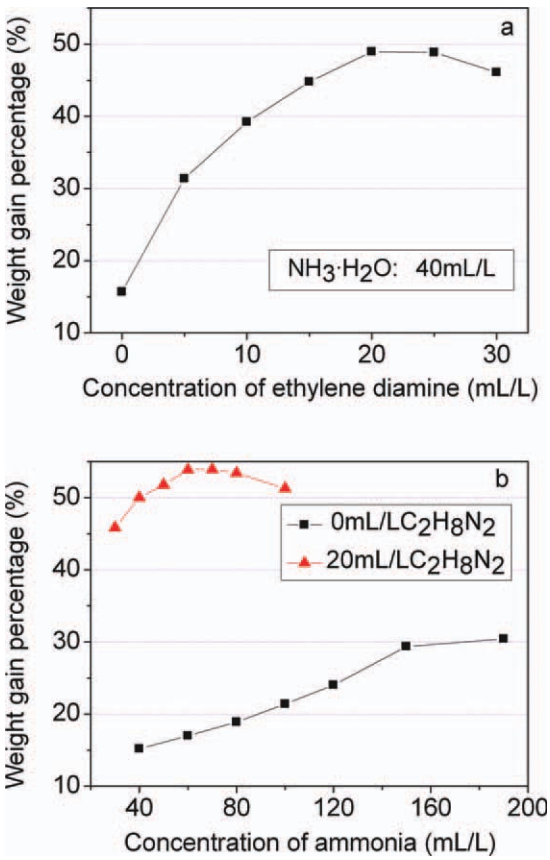

Figure 2 Effect of ethylene diamine on silver weight gain percentage. (a) A fixed concentration of ammonia (40 mL/L) and (b) increasing ammonia concentration with and without ethylene diamine (20 or 0 mL/L). [Color figure can be viewed in the online issue, which is available at wileyonlinelibrary.com.]

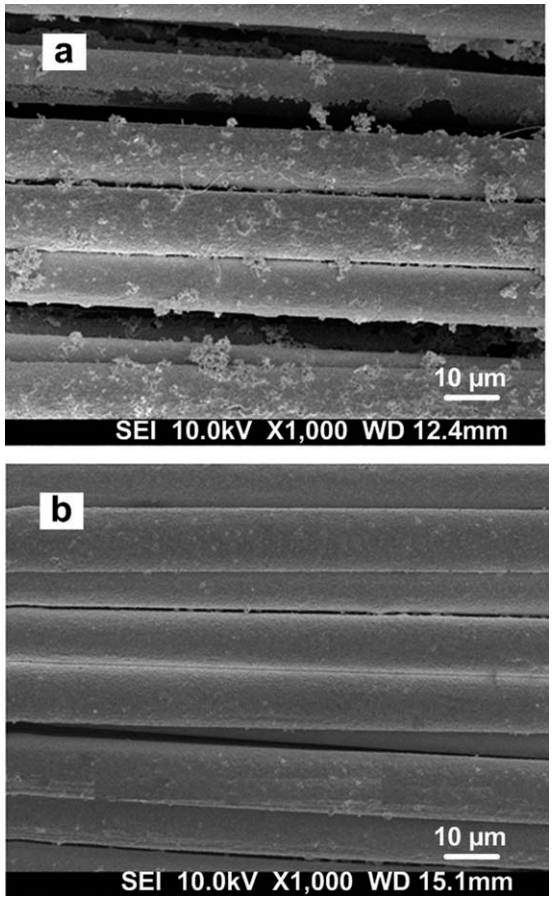

Figure 3 SEM photographs of silver deposits obtained with and without ethylene diamine. (a) 40 mL/L ammonia and (b) 40 mL/L ammonia and 20 mL/L ethylene diamine.

$$D = \frac{k\lambda}{\beta_{1/2}\cos\theta} \tag{2}$$

$$\mathrm{TC} = \frac{I(hkl)/I_0(hkl)}{\sum I(hkl)/I_0(hkl)} \times 100 \tag{3}$$

where $k = 0.89$, $\lambda = 0.154$ nm (Cu Kα radiation), $\beta_{1/2}$ is the width at the half of the height of the diffraction peaks for the crystal plane, and θ is the diffraction angle. $I(hkl)$ is the relative diffraction intensity obtained from the experiment, and $I_0(hkl)$ is the standard diffraction intensity.

RESULTS AND DISCUSSION

Coarsening function of the *para*-aramid fiber surface

The surface of *para*-aramid without etching [shown in Fig. 1(a)] is smooth and lacking in active groups. This characteristic of *para*-aramid surface results in poor binding strength and difficulty of metal deposition. Therefore, it is necessary to coarsen the *para*-aramid surface to carry out electroless plating smoothly. In the present work, NaH/DMSO (5 g/150 g) was synthesized and used as the coarsening solution. Coarsening temperature was 30°C, and coarsening time was 10min. SEM photographs of *para*-aramid fibers with etching are shown in Figure 1(b). The *para*-aramid displayed uneven surface with a large number of micro-pits and grooves. These created micro-pits and grooves may be related to improving the hydrophilicity of the surface, being beneficial to the subsequent pretreatment of metallization.[12] Furthermore, these created micro-pits and grooves will probably provide the latch effect when metal-particles deposited on the *para*-aramid surface, which is advantageous to the enhancement of the adhesion and the bonding strength between *para*-aramid and metal-deposit.

Effect of adding ethylene diamine acting as one of complexing agents

Generally, the plating solution properties and effectiveness mainly depend on the kind of the complexing agent. Conventionally, ammonia is the complexing agent for the electroless silver plating. However, it is not good enough for the plating solution stability and the silver deposits properties. In the present

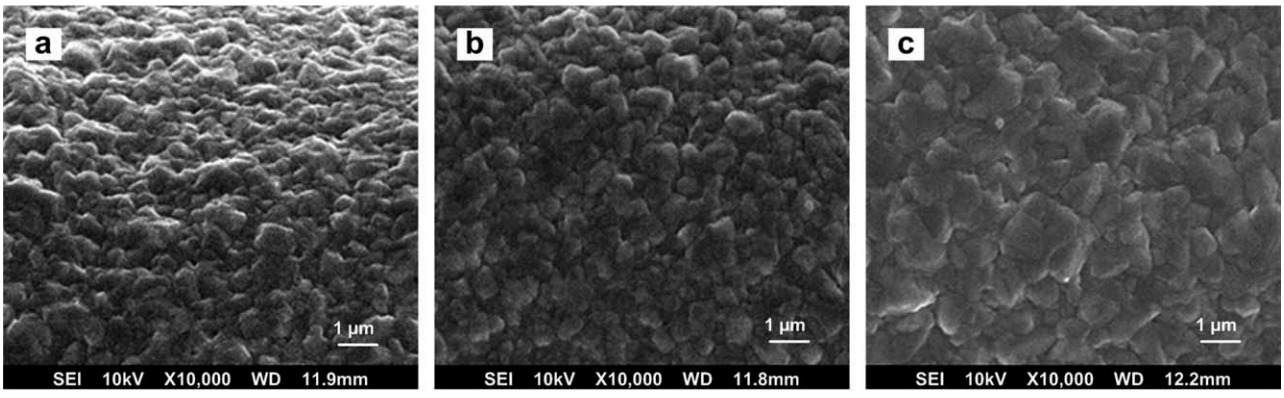

Figure 4 SEM photographs of silver deposits obtained at different concentrations of ethylene diamine: (a) 0 mL/L, (b) 10 mL/L, and (c) 20 mL/L.

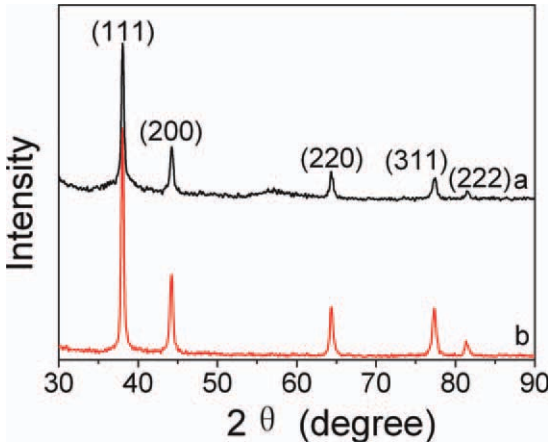

Figure 5 XRD patterns of silver deposits obtained with and without ethylene diamine: (a) 0 mL/L and (b) 20 mL/L. [Color figure can be viewed in the online issue, which is available at wileyonlinelibrary.com.]

work, we used ethylene diamine and ammonia acting as complexing agents together. The effect of ethylene diamine on silver weight gain percentage, surface morphology, and crystal structure of silver deposits was discussed in the next sections.

Effect of ethylene diamine on silver weight gain percentage

Figure 2(a) shows that silver weight gain percentage varied with increasing ethylene diamine concentration at a fixed concentration of ammonia (40 mL/L). It can be seen that silver weight gain was only 15% without ethylene diamine being added into the plating solution. Although the maximum value silver weight gain (~ 50%) was reached when ethylene diamine of 20 mL/L was added. After that, silver weight gain decreased with increasing ethylene diamine concentration. Therefore, ethylene diamine of 20 mL/L was used in this study.

Figure 2(b) shows silver weight gain varied with increasing ammonia concentration with and without ethylene diamine (20 or 0 mL/L). Silver weight gain reached the maximum value (~ 54%) when ammonia concentration was 60 mL/L with a fixed ethylene diamine concentration of 20 mL/L. Meanwhile, silver weight gain reached only ~ 30% when ammonia concentration was increased to 150 mL/L without ethylene diamine.

TABLE III
Crystallite Size and Crystal Plane TC of the Silver Deposits Obtained with and Without Ethylene Diamine

Ethylene diamine (mL/L)	Crystallite size (nm)	TC (%)			
		(111)	(200)	(220)	(311)
0	18.97	28.27	23.33	26.03	22.37
20	22.10	26.17	21.72	26.52	25.59

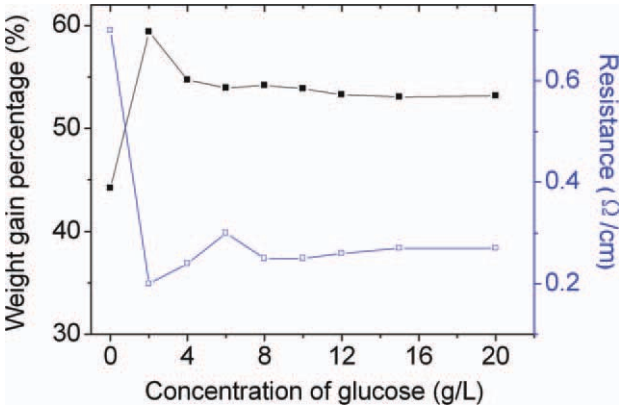

Figure 6 Effect of glucose concentration on silver weight gain percentage and electrical resistance of silver-deposited *para*-aramid fibers. [Color figure can be viewed in the online issue, which is available at wileyonlinelibrary.com.]

Obviously, silver weight gain improved significantly with addition of ethylene diamine in the plating solution, even if ammonia concentration was lower. The reason may be that the complexing ability of ethylene diamine for Ag(I) is stronger than that of ammonia, which reduces the concentration of the silver ion, improves the stability of the plating solution, and decreases the reduction rate of the silver ion. Weight gain reaches the maximum value when the reduction rate approaches the critical deposition rate. The higher silver weight gain is advantageous to a higher conductivity of the silver-deposit *para*-aramid.

Effect of ethylene diamine on surface morphology of silver deposits

SEM photographs of silver deposits with and without ethylene diamine in the plating solution were shown in Figure 3. In Figure 3(a), the deposit was rough and did not cover the total fiber surface.

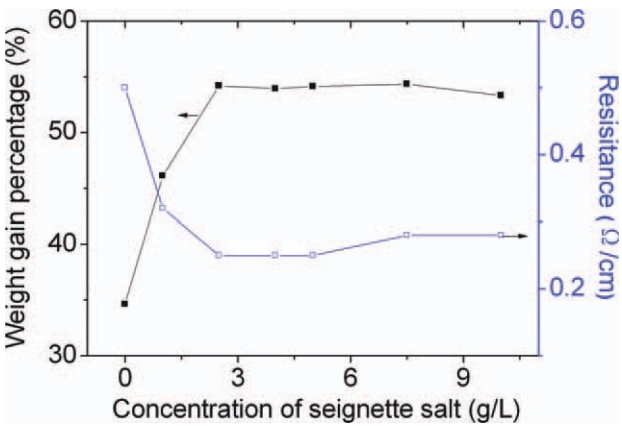

Figure 7 Effect of seignette salt concentration on silver weight gain percentage and electrical resistance of silver-deposited *para*-aramid fibers. [Color figure can be viewed in the online issue, which is available at wileyonlinelibrary.com.]

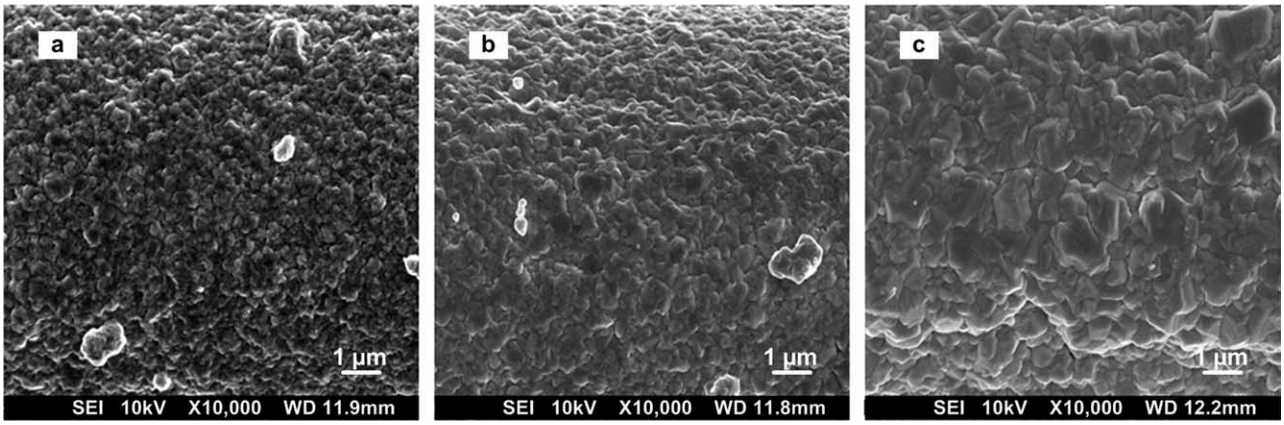

Figure 8 SEM photographs of silver deposits obtained using various reducing agents. (a) 8 g/L glucose, (b) 8 g/L glucose + 2.5 g/L seignette salt, and (c) 2.5 g/L seignette salt.

Many flocculent particles were present. In Figure 3(b), with ethylene diamine being added into the plating solution, the deposit surface became compact and uniform, and the fiber was totally covered.

SEM photographs of the silver deposits at different ethylene diamine concentrations (0, 10, and 20 mL/L, respectively) were shown in Figure 4. As shown in Figure 4(a–c), the grain size became larger (200–500nm), and the deposit became more compact with increasing ethylene diamine concentration.

It is clear that ethylene diamine improved surface morphology of the deposits. The reason is similar to the above-mentioned. The complexing ability of ethylene diamine with Ag(I) is stronger than that of ammonia with Ag(I). This increased the stability of plating solution and decreased silver deposition rate, which was advantageous to produce silver deposits with higher crystalline and perfect structure.

Effect of ethylene diamine on crystal structure of silver deposits

XRD patterns of the silver deposits obtained with and without ethylene diamine are shown in Figure 5. The peaks at $2\theta = 38.0°$, 44.2°, 64.3°, 77.4°, and 81.5° represent (111), (200), (220), (311), and (222) planes of silver, respectively. The silver oxide phase was not detected in the deposits. Figure 5 also shows that the relative peak became sharp and the peak width became narrow slightly, indicating that the crystalline structure of the silver deposits was more perfect.

Crystallite size and crystal plane TC of the silver deposits obtained with and without ethylene diamine are reported in Table III. The result shows that the crystallite size increased slightly (18.97–22.10 nm). This tendency shows an agreement with the change in grain size (illustrated in Fig. 4). Meanwhile, there is insignificant change in plane orientation of silver deposits as listed in Table III.

Effect of two reducing agents on electroless silver plating

Reducing agent is one of the main factors influencing electroless deposition. Glucose and seignette salt are the common reducing agents for the electroless silver plating, respectively. In the present work, we used glucose and seignette salt acting as the reducing agents together. The effect of two reducing agents on silver weight gain percentage, electrical resistance, surface morphology, and crystal structure of silver deposits was discussed in the next sections.

Effect of two reducing agents on silver weight gain percentage and electrical resistance

Figure 6 shows the effect of glucose concentration on silver weight gain percentage and electrical resistance with a fixed seignette salt concentration of 2.5 g/L. A maximum silver weight gain of ~ 59.4% was

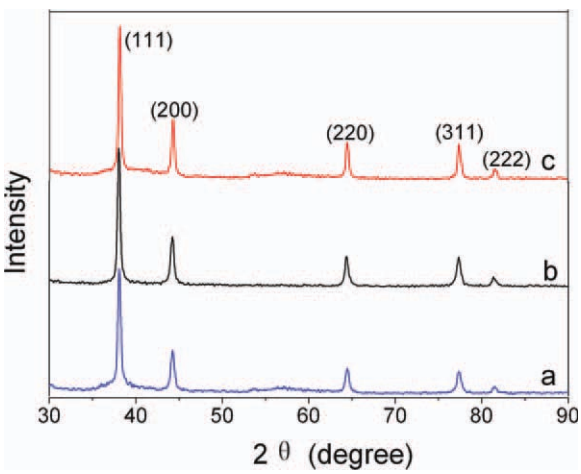

Figure 9 XRD patterns of silver deposits obtained using various reducing agents: (a) 8 g/L glucose, (b) 8 g/L glucose + 2.5 g/L seignette salt, and (c) 2.5 g/L seignette salt. [Color figure can be viewed in the online issue, which is available at wileyonlinelibrary.com.]

TABLE IV
Crystallite Size and Crystal Plane TC of the Silver Deposits Obtained from the Plating Solution with Different Reducing Agents

Concentration of glucose (g/L)	Concentration of seignette salt (g/L)	Crystallite size (nm)	TC (%)			
			(111)	(200)	(220)	(311)
8	0	20.58	27.44	21.57	26.60	24.39
8	2.5	22.10	26.17	21.72	26.52	25.59
0	2.5	24.09	24.27	20.98	29.40	25.35

reached, and the corresponding electrical resistance reached the lowest (0.2 Ω/cm) when a glucose concentration was 2 g/L. Silver weight gain reduced and electrical resistance increased slightly with increasing glucose concentration continuously. Silver weight gain and electrical resistance became stable when glucose concentration was 8 g/L. Therefore, 8 g/L glucose concentration was used in the present work.

Figure 7 shows the effect of seignette salt concentration on silver weight gain percentage and electrical resistance when glucose concentration was fixed at 8 g/L. Silver weight gain was maximum (~ 54%), and electrical resistance was the lowest (0.25 Ω/cm) when the concentration was 2.5 g/L. With further increase in seignette salt concentration, the data also indicate an insignificant change in the silver weight gain and electrical resistance. Therefore, 2.5 g/L seignette salt concentration was used in the present work.

On the whole, silver weight gain improved significantly and electrical resistance of the silver deposits decreased substantially with increasing concentration of the reducing agents. Once a certain concentration range was reached, silver weight gain and electrical resistance became stable. The reduction rate of the silver ion may be first to improve evidently with increasing concentration of the reducing agents. Consequently, silver weight gain increased markedly, resulting in silver deposits resistance decreased. However, when the concentration of the reducing agents reached a certain range, silver deposited on *para*-aramid fibers would tend toward equilibrium. At the current situation, silver weight gain and electrical resistance of silver deposits became stable.

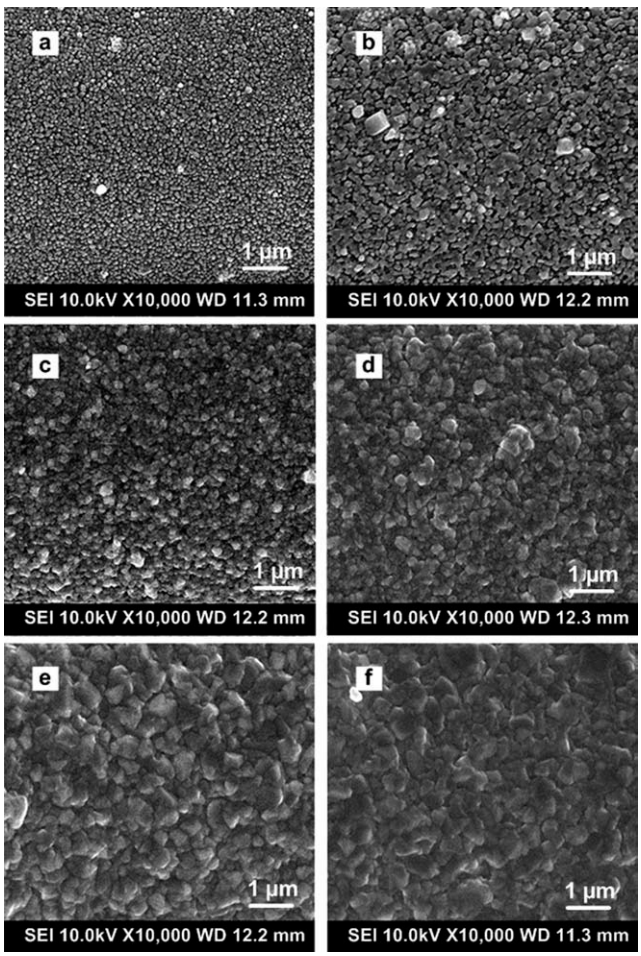

Figure 10 Surface morphology of silver deposits at different plating times: (a) 1, (b) 1.5, (c) 2, (d) 10, (e) 20, and (f) 60 min.

Effect of two reducing agents on surface morphology of silver deposits

SEM photographs of the silver deposits obtained using various reducing agents are presented in Figure 8. In Figure 8(a; only 8 g/L glucose as reducing agent), the deposit was relatively even and compact. The grain size was the smallest (200–250 nm). Thus, the interface and surface area were relatively large.

TABLE V
Relevant Parameters of the Silver Deposits at Different Plating Times

Plating time (min)	Crystallite size (nm)	Grain size (nm)	Color of deposit
1	14.64	50–70	Black
1.5	16.82	120–140	Black
2	17.59	160–180	Black
10	22.10	230–250	Silver gray
20	22.10	350–400	White
60	22.10	430–470	White

Figure 11 Appearance of silver deposits on *para*-aramid fibers. [Color figure can be viewed in the online issue, which is available at wileyonlinelibrary.com.]

This influenced the electrical and corrosion resistance of the silver deposits.

In Figure 8(c; only 2.5 g/L seignette salt as reducing agent), the grain size was the largest (500–550 nm). The deposit was uneven and relatively rough. This resulted in higher electrical resistance and lower corrosion resistance of the deposits.

In Figure 8(b; 8 g/L glucose and 2.5 g/L seignette salt as reducing agents together), the deposit was even and compact. The grain size was also relatively large (370–450 nm). This contributed to the reduced electrical resistance and increased corrosion resistance of the deposits.

Effect of two reducing agents on crystal structure of silver deposits

XRD patterns of the silver deposits obtained using various reducing agents are shown in Figure 9. Based on the parameter information in Figure 9, the crystallite size and crystal plane TC of the silver deposits were calculated and listed in Table IV. The crystallite size was the smallest (20.58 nm) with only glucose acting as the reducing agent. It was the largest (24.09 nm) with only seignette salt acting as the reducing agent. It was a middle value (22.10 nm) with glucose and seignette salt acting as the reducing agents together. This tendency shows an agreement with the change in grain size (illustrated in Fig. 8). Meanwhile, there is an insignificant change in plane orientation of silver deposits as given in Table IV.

Effect of plating time on growth morphology of silver deposits

Figure 10 illustrates the surface morphology of silver deposits at different plating durations. Commonly, electroless plating deposits were considered the three-dimensional nucleation and growth model (Volmer–Weber).[13] The deposition occurred at the most active point and became isolated island [shown in Fig. 10(a)]. And then, these small islands began to grow large from three-dimensional directions and became network structure to attach a connection between island and island [shown in Fig. 10(b,c)]. After that, the network space gradually filled in and became continuous deposition layers. Meanwhile, silver deposit thickness increased [shown in Fig. 10(d–f)] and silver deposits appeared black, silver gray, and white in turn.

Table V gives the relevant parameters of silver deposits at different plating times. It can be seen that when the plating times were 1, 1.5, and 2 min, the crystallite and grain sizes increased. At first, the grain size was less than the wavelength of visible light (380–780 nm), which made the deposit appear black. At 10, 20, and 60-min plating times, the crystallite size was 22.10 nm, but the grain size is still increasing. At 10-min plating time, the grain size was 230–250 nm, and the deposits were silver gray. At longer plating times, larger grain sizes (350–470 nm) were obtained, and the deposits appeared white (shown in Fig. 11).

Mechanical properties of silver deposit *para*-aramid

Mechanical properties of the electroless silver deposited *para*-aramid fibers are reported in Table VI. The breaking strength of the silver deposit *para*-aramid fibers was 44.0 N, and the strength retention reached values of up to 95.6%.

In the present work, the breaking strength of fibers decreased 6% after *para*-aramid surface was

TABLE VI
Mechanical Properties of the Etched and the Silver Deposit *Para*-Aramid Fibers

	Blank fibers	Etched *para*-aramid fibers	Silver deposit *para*-aramid fibers	Test standard
Breaking strength (*N*)	46.0	43	44.0	GB/T 14344–2008
Elongation (%)	3.0	–	2.9	

coarsened. However, Table VI shows that the breaking strength was reduced by only 4.4% for the silver deposit *para*-aramid fibers.

The slight increase in the breaking strength compared to that of the surface-coarsened *para*-aramid fibers maybe results from the silver deposits of which the lattice array also makes a little contribution to the breaking strength. This effect was advantageous, leading to slight increase in the breaking strength of fibers. On the whole, silver deposit *para*-aramid fibers still retained high strength (44 N).

CONCLUSIONS

Electroless silver plating on *para*-aramid fibers and growth morphology of silver deposits was investigated. Etching the surface of *para*-aramid using NaH/DMSO coarsening solution was found to be necessary to guarantee successful electroless plating, because the *para*-aramid surface was smooth and lacking in active groups. Two complexing agents (ethylene diamine/ammonia) and two reducing agents (glucose/seignette salt) were used for the electroless silver plating bath design.

Silver weight gain increased markedly with the addition of ethylene diamine to the plating solution, even if ammonia concentration was lower. Ethylene diamine improved the surface morphology. Crystallite and grain sizes increased slightly, and there was insignificant change in plane orientation of the silver deposits. Silver weight gain was maximum value, and electrical resistance was the lowest when 8 g/L glucose and 2.5 g/L seignette salt were used as the reducing agents together. The resulting deposits were even and compact, the crystallite and grain sizes were relatively large, and there was insignificant change in plane orientation of the silver deposits.

Electroless silver plating deposits were considered to be three-dimensional nucleation and growth model (Volmer–Weber). Black, silver gray, and white deposits appeared sequentially with progressive plating. The crystallite and grain sizes increased with increasing plating time. In addition, the prepared silver deposit *para*-aramid fibers showed high strength (44 N).

References

1. Burch; Robert, R.; Hsu; Che, H. U. S. Pat.5,773,089 (1998).
2. Gabara; Hsu, V.; Tokarsky, C. H.; Edward, W. U. S. Pat. 5,302,415 (1994).
3. Hsu, C. WO 9,534,707-A1 (1995).
4. Hsu, C. U. S. Pat. 5453299-A (1995).
5. Zhao. X.; Hirogaki, K.; Tabata, I.; Okubayashi, S. Surf Coat Technol 2006, 201, 628.
6. Burch; Robert, R. G.; Richard, L.; Phillips, K. S.; Brian, R. U. S. Pat. 5,370,934 (1994).
7. Kosuga, K.; Watanabe, M.; Yamamoto, T. Jpn Pat. 135,526-A (2009).
8. Banaszczyk, J.; Schwarz, A.; Mey1, G. D.; Langenhove, L. V. J Appl Polym Sci 2010, 117, 2553.
9. Schwarz, A.; Hakuzimana, J.; Westbroek, P. Proceedings of the 6th international workshop on wearable and implantable body sensor networks. Berkeley, Computer Society press, CA 2009; p 278.
10. Gasana, E.; Westbroek, P.; Hakuzimana, J. Surf Coat Technol 2006, 201, 3547.
11. Schwarz, A.; Hakuzimana, J.; Kaczynska A.; Banaszczyk, J.; Westbroek, P. Surf Coat Technol 2010, 204, 1412.
12. Luan, B.; Yeung, M.; Wells, W. Appl Surf Sci 2000, 156, 26.
13. Yang, B. Z. Master Dissertation, Jilin University (in Chinese) 2007.